A III-V pin- photodetector array with high responsivity and bandwidth for radio over free space optical communication

G. Morthier, Y. Yan, J. Van Kerrebrouck, N. Singh, Y. Liu, H. Salmanian, Z. Wu, M.S. Zhao

***Abstract*—**We discuss the performance of a photodetector array for use in radio over free space optics. Radio over free space optics (RoFSO) combines high bandwidth with flexibility and is a highly desired wireless communication option in 5G and 6G networks. For all elements of the array, we demonstrate 10 Gb/s operation with very low bit-error-rate for both NRZ and PAM-4 modulation. Transmission over both fiber and free space are reported.

***Index Terms*—photodetector array, free space optical communications, high bitrate operation**

I. INTRODUCTION

Radio over optical communications provides higher bandwidth, has lower sensitivity to electro-magnetic radiation and is more secure than traditional RF-communication. It is therefore important for the introduction of 5G and 6G mobile communications [2,3] It is mostly implemented using fiber-optic transmission. However, in places where fiber installation is not cost-effective or fiber has not been installed yet, e.g., in rural areas, radio over free space optical (RoFSO) communication might be preferred. A disadvantage of free space optical communication is that it requires a line of sight to be maintained though, and that it is prone to atmospheric interference [4]. To guarantee this, a wide field of view is indispensable.

Such wide fields of view (Fov) can be obtained with arrays of grating couplers coupled to waveguide photodetectors [6] or by arrays of surface photodetectors. Grating couplers are unfortunately polarization dependent whereas surface photodetectors don't suffer from that dependence. PD arrays (PDAs) also offer better detection efficiency over a broad range of incidence angles and thus have wider FoV.

Here we consider back-illuminated InP/InGaAs p-i-n PDAs with high responsivity in the C-band of 1 A/W and low dark current under 0.35 nA (see [1]).

G. Morthier, J. Van Kerrebrouck, N. Singh, and H. Salmanaian are with the Department of Information Technology, Ghent University - imec, Technologiepark-Zwijnaarde 126 B-9052, Ghent, Belgium (e-mail: geert.morthier@ugent.be). Y. Yan, Y. Liu, Z. wu and M.S, Zhao are with the School of Optoelectronic Engineering and Instrumentation Science, Dalian University of Technology, 116024 Dalian, China.

979-8-3195-4420-9/26/$31.00 ©2026 IEEE

Below we discuss the characteristics of the PDA and its performance in digital communication experiments. The entire PDA was mounted on a PCB and wire bonded for the transmission experiments. The PCB was also optimized for high speed operation. It is noted here that while the PDA can serve as receiver with large FoV for a single free space channel, it could also serve as receiver for spatially multiplexed channels, where each spatial channel addresses a different PD.

II. DESIGN AND CHARACTERISTICS OF THE PDA

In free space optical communication, the spot size of the beam is usually larger than the spot size of a beam from a single mode fiber. For this reason, the PDs should have a relatively large diameter. However, as there is also a trade-off with the parasitic capacitance and bandwidth of the PDs, we opted for a PD array with each PD having a diameter of 50 µm. The PDs are back illuminated and consist of an InGaAs-based III-V material stack, forming a PIN structure and grown using MOVPE on a n-type InP substrate. A sketch of the PDA and an illustration of the fabrication process are shown in Figure 1.

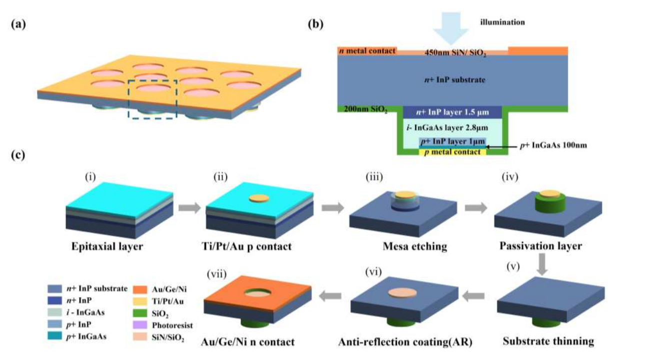

Fig. 1. Schematic diagram of the vertical back-illuminated structure of the PDA. (a) PIN PDA with a common cathode.(b) Cross-section of the single photodetector in the PDA. The photocurrent and dark current are fully collected by the n-metal contact and p-metal contact.(c) Vertical back-illuminated PDA fabrication process.

The responsivity, dark current and frequency response of the different PDs from the array were measured at room temperature and at a wavelength of 1550nm. Dark current and responsivity are shown in Figure 2. One can observe the high responsivitiy, slightly above 1 A/W for all PDs, and low dark current, below 0.35 nA at a bias voltage of -5V and down to

0.15 nA for lower bias voltages. The static characteristics are in general quite uniform over all 10 PDs from the array.

The PDA was then wire-bonded and assembled on a planar circuit board (PCB) and wire bonded, as shown in Figure 3. This initially led to a bandwidth of 1.8 GHz. The design of the PCB was subsequently optimized and the maximum modulation bandwidth was increased by this optimization to 2.7 GHz, with also a flatter response in general and, e.g., a 6 dB bandwidth that was increased from 3 to 5GHz from first to second iteration. Figure 4 shows the S_{21} characteristics of the different elements in the array vs the modulation frequency.

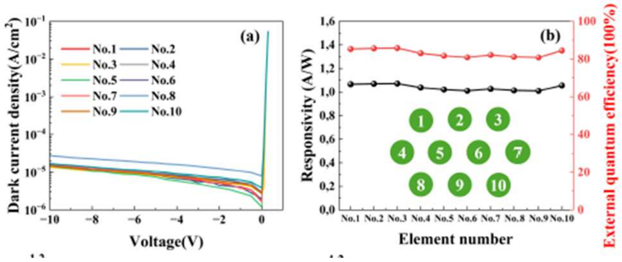

Fig. 2. The performance characteristics of each element in the PDA. (a) The dark current and dark current density for all elements. (b) The responsivity for all PD elements and their calculated EQE..

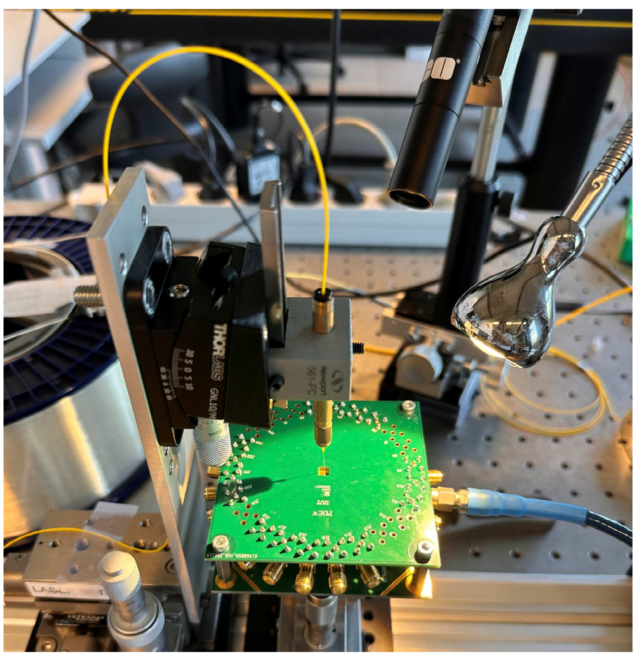

Fig. 3. Photograph of the fabricated PDA, assembled on a PCB.

III. FIBER-OPTIC LINK EXPERIMENTS

First link experiments were done over standard single mode optical fiber, using the set-up shown in Figure 5. Fibers of both 2km and 25km length were used in the experiments and in the latter case also an EDFA was inserted in the link right after the transmitter. Taking advantage of the slow decay of the S21 response, we managed to show very low bit-error-rates (BERs) up to 10 Gb/s by applying zero forcing equalization at the transmitter side, and this for both NRZ-OOK and NRZ-PAM-4 signals.

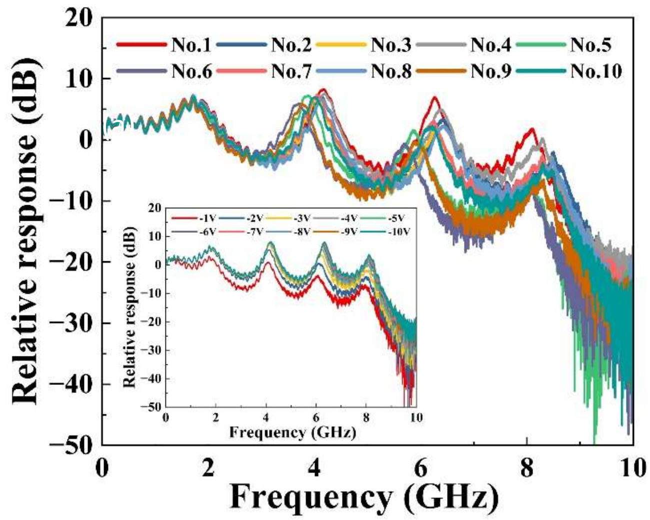

Fig. 4. S_{21} characteristics of the different photodiodes in the array after assembly on a PCB, for a reverse bias voltage of 5V. Inset: S_{21} characteristics of photodiode No. 1 for different bias voltages.

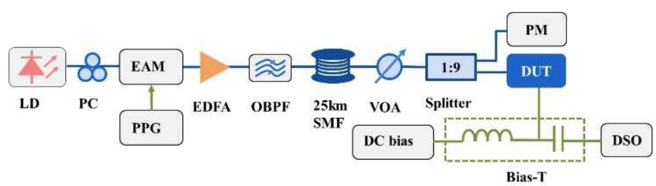

Fig. 5. Measurement setup for the fiber-optic link experiments

Figures 6 and 7 show the eye diagram for both 10 Gb/s NRZ-OOK and 10 Gb/s NRZ-PAM-4 modulation after propagation over 25 km of SSMF. For the NRZ-OOK signal, the Q measured by the DSO is 7.94, corresponding with a BER of 10^{-12}. Figure 8 shows the measured BER values vs. received optical power for all 10 elements, for 10 Gb/s NRZ-OOK modulation. One can see that for all PDs of the array, a BER below 10^{-12} can be achieved. This was also the case for the 2 km link without EDFA.

Further increases of the maximum speed of the PDA are expected by reducing the transit time in the absorbing layer (currently with a thickness of 2.8 μm), but this would also affect the responsivity and efficiency somewhat.

IV. FREE SPACE TRANSMISSION EXPERIMENTS

To realize a low cost FSO receiver for short range wireless communication, an architecture consisting of the PDA and a condenser lens, without active optical beam tracking, was set up and studied. This setup was simulated first and is shown in Figure 9.

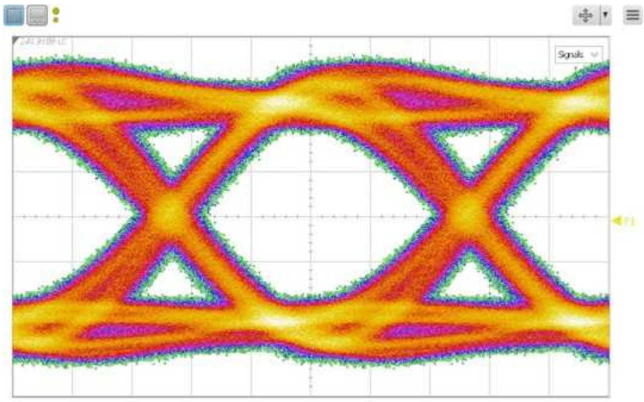

Fig. 6. Eye diagram for 10 Gb/s NRZ modulation after propagation over 25 km of SSMF. The Q measured by the DSO is 7.94, corresponding with a BER of 10^{-12}.

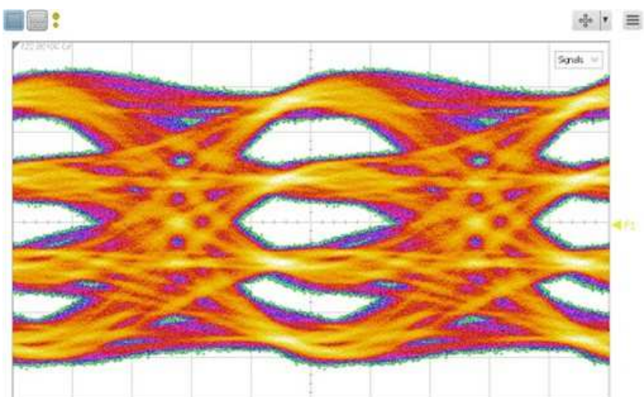

Fig. 7. Eye diagram for 10 Gb/s PAM-4 modulation (5GBd) after propagation over 25 km of SSMF.

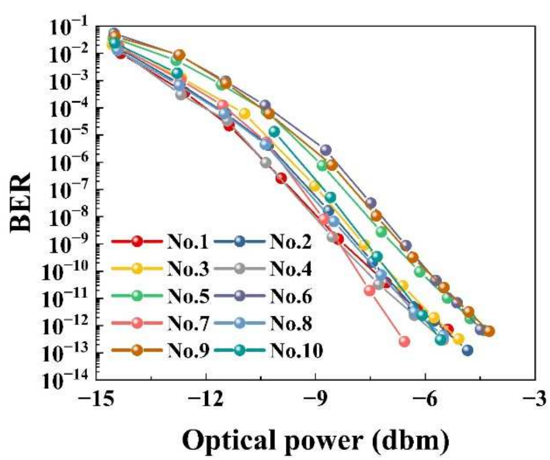

Fig. 8. BER vs received optical power at 10Gb/s for all 10 pixels.

At the transmitter side, the optical signal first propagates through 25 km of single mode fiber (SMF) and is then collimated into free space by a fiber collimator. After free space propagation, a condenser lens collects and focuses the beam onto the PDA. The whole system was analysed numerically using Gaussian beam theory as well ray tracing with the Ansys Zemax Optic Studio [9].

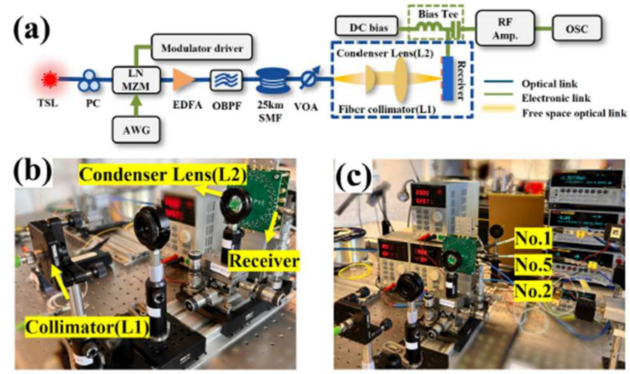

Fig. 9. (a) Experimental setup for RoFSO communication using the PDA as receiver. The blue, green and orange lines represent the electrical, optical and free space optical links, respectively. (b) The free space light direct coupling in the receiver. (c) The different elements in the PDA measured at the same time.

If the PDA is positioned in the focal plane of the condenser lens, then the focused spot will overlap with the photosensitive area and all light is converted by the photodetector. However, it is also important to know the alignment tolerance for free space communication. This alignment tolerance was measured experimentally. Figure 10 gives the alignment tolerance by means of the photocurrent variation along the axis. The photocurrent remains obviously constant as long as the spot diameter on the PDA remains below the 50 mm photosensitive area of each PD. The broad flat region around 5mm indicates a strong tolerance for axial misalignment.

Important is finally the crosstalk in the case of multi channel systems, with each PD of the PDA meant to receive a different spatial channel. Fig. 11 shows the small signal crosstalk measurements as a function of modulation frequency. The central PD was illuminated and was the destined receiver for the free space communication channel, while the nearest neighbours (No.1, No.2, No.4, No.6, No.8 and No.9) and secondary (No.7) adjacent channels serve as the probe channels for crosstalk assessment. The crosstalk on all measured channels was estimated to be approximately -30 dB below the main signal (No.5) at 2.8 GHz (3 dB bandwidth). This confirms that crosstalk is negligible and that multiple channels can reliably transmit signals in parallel.

Under large signal, digital modulation, the different PDs of the array also operated error free (with BER numbers below 10^{-12}) for a free space optical link after the fiber. For this case, we also investigated higher bitrates, up to 20 Gbps. The obtained BER vs bitrate are shown in Figure 12 for element 1. One can see that up to 20 Gbps, the BER is still below the SD-FEC (Soft Decision Forward Error Correction) limit.

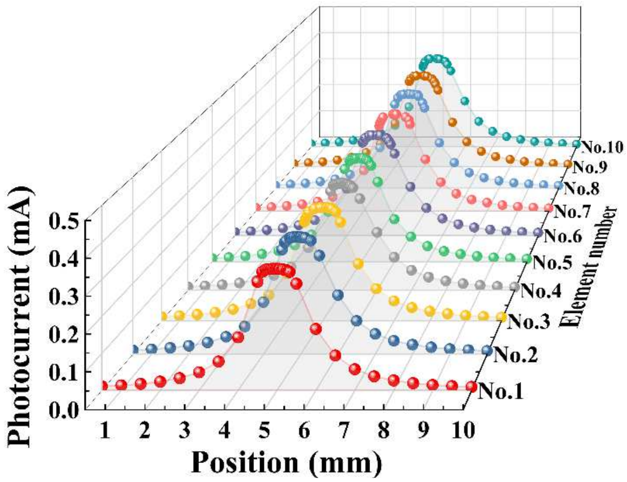

Fig. 10. The z axis optical alignment profile for the 10-element PDA.

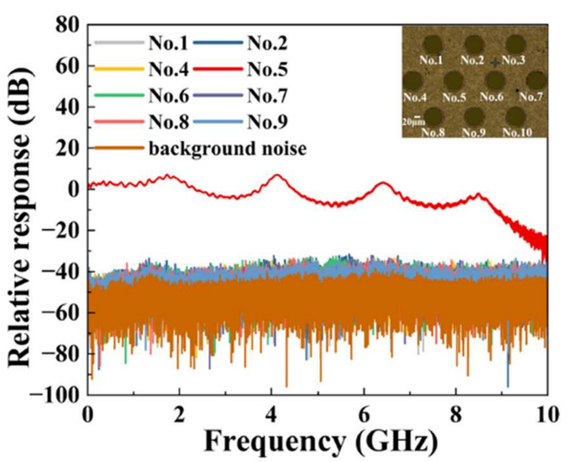

Fig. 11. The crosstalk between element No. 5 and the nearest and secondary neighboring elements were measured simultaneously.

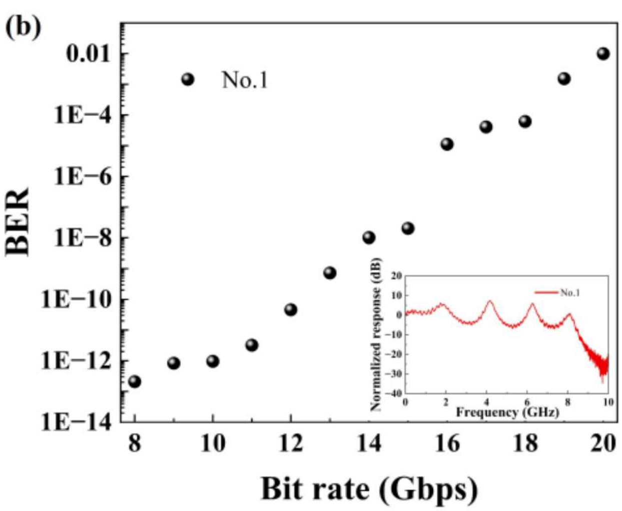

Fig. 12. BER of element 1 vs. bitrate ..

V. CONCLUSION

We have described a photodetector array based on the InP/InGaAs material with high responsivity, low dark current and high modulation bandwidth for each photodetector. The array has been wire bonded and mounted on a PCB, which was itself also optimized for high speed operation.

We demonstrated high speed optical transmission for the array. After mounting, each detector in the array is capable of working up to 10 Gb/s, using FFE at the transmitter side. Transmission over 2 and 25 km of single mode fiber was done to mimic free space optical transmission. We also demonstrated free space optical transmission over …

ACKNOWLEDGMENT

The authors thank Dr. Clemens J. Krückel, Ing. Steven Verstuyft and Dr. Yujie Guo for technical support and the BOF fund of Ghent University for financial support.

REFERENCES

[1] Y. Yan, M. Yang, S. Han, C. Kang, H. Salmanian, Z. Wu, Y. Gu, M. Zhao, G. Morthier, 'Multi channel RF optical receiver enabled by a high performance p-i-n InP-InGaAs based photodetector array', Opt. Lett., Vol. 50, N08, 3 April, 2025.

[2] T. Imai, N. Shibata, S. Kaneko, R. Hamagami, J. Kani, T. Yoshida, 'Tracking based on control information and beam divergence control in FSO with moving nodes toward 6G', IEICE Commun. Express **12(9)**, pp. 547-552, 2023.

[3] H.-H. Lu, X.-H. Huang, W.-S. Tsai, C.-Y. Feng, Y.-T. Huang, A. Nainggolan, '800 Gb/s/200 m FSO link with a WDM-PAM4 scheme and SLM-based beam tracking technology', Opt. Lett. **46(6)**, pp. 1269-1272, 2021.

[4] A. Prokes, 'Atmospheric effects on availability of free space optics systems', Optical Engineering **48(6)**, art. 066001 , 2009.

[5] A. Bekkali, M. Hattori, Y. Hara, and Y. Suga, "Free space optical communication systems for 6G: A modular transceiver design," IEEE 296 Wirel. Commun. **30(5)**, pp. 50–57, 2023.

[6] F. Aflatouni, B. Abiri, A. Rekhi, and A. Hajimiri, 'Nanophotonic projection system', Opt. express **23(16)**, pp, 21012-21022, 2015.

[7] C. Xue, H. Xue, B. Cheng, W. Hu, Y. Yu and Q. Wang, "1×4 Ge-on-SOI PIN Photodetector Array for Parallel Optical Interconnects," J. Light. Technol. **27(24)**, pp. 5687–5689, 2009.

[8] Y. Yan, J. Van Kerrebrouck, N. Singh, H. Salmanian, M.X. Yang, Z. Wu, M.S, Zhao, G. Morthier, 'Optical signal acquisition using an alignment robust receiver based on photodetector array', Optics Letters **50**(23), pp. 7199-7202, 2025

[9] ZEMAX, Ánsys Zemax Opticstudio', https://www.ansys.com/zh-cn/products/optics/ansys-zemax-opticstudio..